Relativity tests by complementary rotating Michelson-Morley experiments

Holger Müller*
Physics Department, Stanford University, 382 Via Pueblo Mall, Stanford, California 94305, USA

Paul Louis Stanwix, Michael Edmund Tobar, Eugene Ivanov
University of Western Australia, School of Physics M013, 35 Stirling Hwy., Crawley 6009 WA, Australia

Peter Wolf
LNE-SYRTE, Observatoire de Paris, 61 Av. de l'Observatoire, 75014 Paris, France

Sven Herrmann, Alexander Senger, Evgeny Kovalchuk, and Achim Peters
Institut für Physik, Humboldt-Universität zu Berlin, Hausvogteiplatz 5-7, 10117 Berlin, Germany
(Dated: February 16, 2013)

We report Relativity tests based on data from two simultaneous Michelson-Morley experiments, spanning a period of more than one year. Both were actively rotated on turntables. One (in Berlin, Germany) uses optical Fabry-Perot resonators made of fused silica; the other (in Perth, Australia) uses microwave whispering-gallery sapphire resonators. Within the standard model extension, we obtain simultaneous limits on Lorentz violation for electrons (5 coefficients) and photons (8) at levels down to 10^{-16}, improved by factors between 3 and 50 compared to previous work.

PACS numbers: Valid PACS appear here

arXiv:0706.2031v1 [physics.class-ph] 14 Jun 2007

The original Michelson-Morley (MM) experiment provided physicists with a first glimpse of Lorentz invariance when relativistic velocities were inaccessible to experiments and the theory of relativity was yet to be formulated. In a similar way, modern versions of outstanding precision can attempt to detect minuscule *violations* of Lorentz invariance and thus provide physicists with a first glimpse of effects of a future theory of quantum gravity in the low-energy limit [1, 2, 3]. Since the form of the putative violations is not predetermined, it is important to probe a broad variety of them experimentally.

In contrast to the original interferometer experiments [4], modern MM-experiments are generally based on a measurement of the resonance frequencies

$$\omega = 2\pi \frac{mc}{2nL} \tag{1}$$

(m is a constant mode number, c the velocity of light, and n the index of refraction if a medium is present) of standing waves in resonant optical or microwave cavities. Any type of Lorentz violation that affects the isotropy of c [5], L [6, 7, 8], or n [8] can potentially be detected. L and n are properties of macroscopic matter and thus sensitive to Lorentz violation in the Maxwell and Dirac equations that govern its constituents. However, each of the simple MM-experiments performed so far (recently, [9, 10, 11, 12, 13, 14, 15, 16, 17]) does not by itself provide enough information to distinguish between the different influences and thus can only bound combinations of them. To remove these restrictions, experiments featuring dissimilar cavities that have a different dependence of L and n on Lorentz violation have been suggested [7, 8].

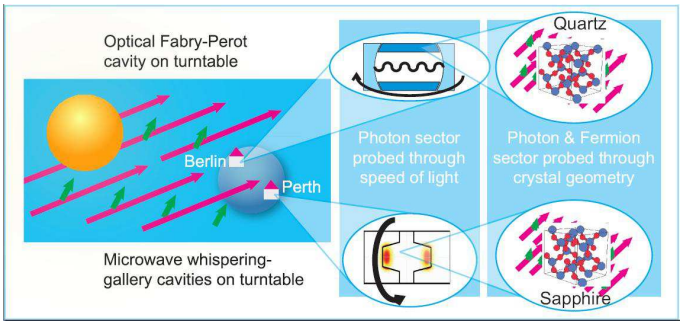

FIG. 1: Modifications of c, n, and L are probed for cavities of different geometry and material, which allows us to separately probe Lorentz violation in the electron and photon sector (symbolized by the arrows).

Here, we report on the first realization of such simultaneous, complementary MM-experiments that use different cavity materials, geometries, operating frequencies, and locations (Berlin, Germany and Perth, Australia) in different hemispheres (Fig. 1). Both provide data spanning a period of more than one year and were performed on a rotating table. This allows us to use Earth's orbital motion and rotation, as well as the turntables, to modulate the 'laboratory' frame of reference and thus to restrict Lorentz violations of more general symmetries than otherwise possible. By combining all data, we obtain independent, simultaneous limits on a broader range of Lorentz violations in the Dirac and Maxwell sectors than any single experiment could.

We use the standard model extension (SME) [18] as a comprehensive framework for Lorentz violation. It ex-

*Electronic address: holgerm@stanford.edu

tends the Lagrangians of the standard model by the most general Lorentz violating terms that can be formed from the standard model fields and Lorentz tensors. Modifications of the photon sector [5, 19] are described by a tensor $(k_F)_{\kappa\lambda\mu\nu}$ entering the Maxwell equations. Ten of its elements lead to a dependence of c on the polarization. The observation that the apparent polarization of certain astronomical sources does not depend on the wavelength bounds them to levels between 10^{-37} and 10^{-32} [2, 5]. The remaining nine elements of $(k_F)_{\kappa\lambda\mu\nu}$ can only be measured in laboratory instruments that probe the isotropy of c. They can be arranged into traceless 3×3 matrices $\tilde{\kappa}_{e-}$ (symmetric) and $\tilde{\kappa}_{o+}$ (antisymmetric) [5]. $\tilde{\kappa}_{e-}$ and $\tilde{\kappa}_{o+}$ also affect L and n due to a modification of the Coulomb potential, but this has been shown to be negligible for most experiments, including ours [6].

Non-negligible shifts in L and n, however, result from Lorentz violation in the electron sector [7, 8, 20]. In the non-relativistic limit, a modification of the electron's energy-momentum relation according to $p^2/(2m) \to (p^2 + p_j p_k E^{jk})/(2m)$ where p is the 3-momentum and $E'_{jk} = -c_{jk} - \frac{1}{2}c_{00}\delta_{jk}$ is given by a SME tensor $c_{\mu\nu}$ that enters the Dirac Lagrangian of the free electron. The resulting modification of the electronic states within solids leads to a change of L that is given by the diagonal elements of a strain tensor

$$e_{jk} = \frac{1}{2}\left(\frac{\partial L_j}{\partial x_k} + \frac{\partial L_k}{\partial x_j}\right) = \mathcal{B}_{jklm}E'_{lm}\,. \qquad (2)$$

The sensitivity tensor $\mathcal{B}$ is predicted in detail by invoking perturbation theory for the electrons as described by Bloch wave functions [7, 8]. This theory also predicts a change of the index of refraction. For materials of trigonal or higher symmetry and microwave frequencies,

$$\frac{\delta n}{n} = \bar{\beta}E'_3, \quad \bar{\beta} = \frac{(n^2-1)(n^2+2)}{3n^2}(\mathcal{B}_{31} - \mathcal{B}_{13}) \qquad (3)$$

and $E'_3 = E'_{11} + E'_{22} - 2E'_{33}$ [8]. Because of the material dependence of $\mathcal{B}$ and $\bar{\beta}$, experiments using cavities of different nature measure independent combinations of the elements of k_F and $c_{\mu\nu}$.

Throughout this work, we use the conventions made in Refs. [7, 8]. In particular, by definition of coordinates and fields, we take the proton sector to be Lorentz invariant. This is always possible [5, 18] and leads to an unambiguous definition of the c- and k_F- coefficients.

If Lorentz invariance is violated, the resonance frequency ω of our cavities will exhibit a measurable modulation having Fourier components at frequencies that are integer combinations of twice the angular frequency of the turntable $2\omega_t$, Earth's rotation $\omega_\oplus$, and Earth's orbit $\Omega_\oplus$. Such a signal can be expressed as $\delta\nu/\bar{\nu} = B\sin 2\omega_t T + C\cos 2\omega_t T$, where

$$\begin{aligned} B = B_0 + B_{s1}\sin\omega_\oplus T + B_{c1}\cos\omega_\oplus T + B_{s2}\sin 2\omega_\oplus T \\ + B_{c2}\cos 2\omega_\oplus T, \quad C = C_0 + C_{s1}\sin\omega_\oplus T \\ + C_{c1}\cos\omega_\oplus T + C_{s2}\sin 2\omega_\oplus T + C_{c2}\cos 2\omega_\oplus T \qquad (4) \end{aligned}$$

are themselves time-dependent. This is a general expression, applicable in any test model that leads to modulation at (some of) these frequencies. In the SME, the B, C will depend on different linear combinations of the elements of k_F and c. By analyzing the measured cavity frequency in terms of the above modulations, separate measurement of the tensor elements is thus possible. An experiment without turntable can measure four combinations. If at least 1 y of data is taken, three additional ones, that depend on the Lorentz boost due to Earth's orbit and cause modulation components differing by $\Omega_\oplus = 2\pi/1\,\mathrm{y}$ in frequency, can be resolved. Finally, use of a turntable provides access to an eighth coefficient, which is otherwise suppressed due to the presence of a symmetry axis (Earth's axis). However, to separately measure the changes in L and n is only possible with complementary experiments that use different cavities and materials.

The Berlin setup compares the resonance frequencies of two monolithic, diode-pumped neodymium:YAG lasers at a wavelength of 1064 nm that are stabilized to resonances of Fabry-Perot cavities fabricated from fused silica (with BK7 substrates for the mirrors). One (L=2.85 cm, Finesse $\mathcal{F} = 1.7\times 10^5$) is continuously rotated at a rate of $1/(43\,\mathrm{s})$. To reduce systematic effects associated with table rotation, a precision air bearing turntable (type RTV 600, Kugler GmbH, Salem, Germany) is used that is specified for $< 0.1\,\mu$rad rotation axis wobble. The rotation axis is actively stabilized to the vertical using a tilt sensor (Applied Geomechanics, Inc.) on the rotating platform. The other cavity (L=10 cm, $\mathcal{F} = 2\times 10^4$) is oriented north-south.

Data has been collected for 396 d, totalling to 62 d of useful data in 27 sets (118,000 turntable rotations), beyond the data already reported in [14]. To analyze the data, we first break it down into $i = 1....N$ subsets of 10 table rotations each. This approaches an optimal filter that rejects possible signal components due to drift of the cavity frequency while passing the sinusoidal signals. The subsets are individually fitted with the sine and cosine amplitudes $B(t_i)$ and $C(t_i)$ (each is taken as constant over the subsets and assigned the subset's mean time t_i). Systematic influences are allowed for in the fit function by including sine and cosine amplitudes at ω_r, a constant offset, and drift terms linear and quadratic in time. This yields 192 values for each of $B(t_i)$ and $C(t_i)$ from each 24 hours of data. Then, the $B(t_i), C(t_i)$ coefficients are fitted with Eq. (4). Performing similar fits on all 27 data sets yields one set of B_k and C_k from each, see Fig. 2.

Residual systematic effects at $2\omega_r$ primarily affect the coefficients C_0 and B_0 at a level of 5σ within individual subsets. They differ in phase and magnitude (see Fig. 2) and average out in the final result. This, however, leaves an increased error bar on the C_0 and B_0 averages. The other amplitudes have relatively smaller error bars, as they are are affected by systematics only indirectly through additional time-dependent influences, such as a

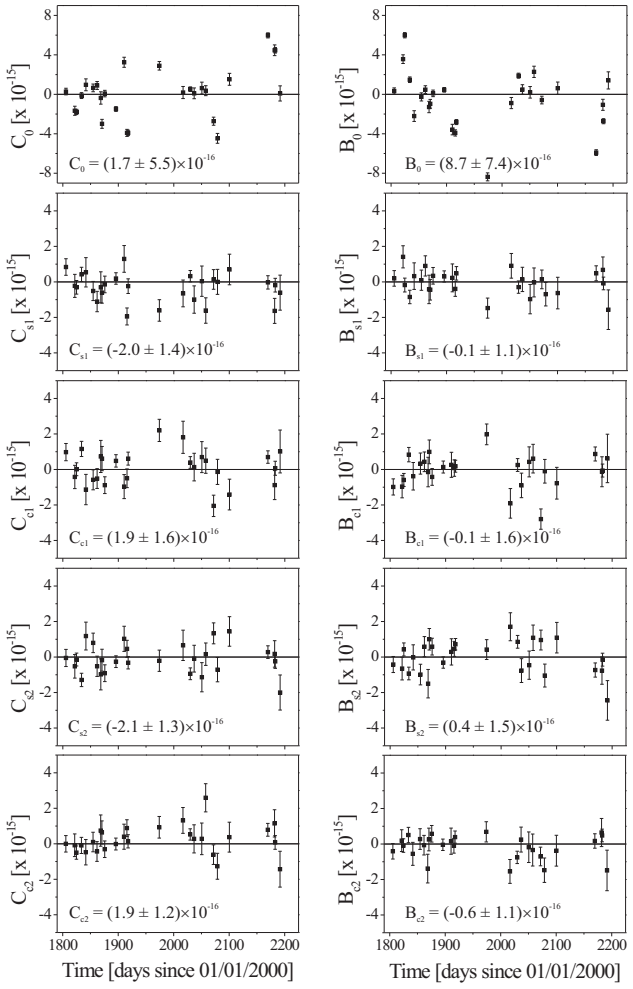

FIG. 2: B_k, C_k versus time.

daily modulation of temperature or tilt of the building floor.

The hypothetical signal for Lorentz violation in the SME, calculated from the motion of the cavities by following the methods described in Refs. [5, 6, 8] is detailed in Tab. I. As throughout the literature, the coefficients for Lorentz violation with capital indices are referred to a sun-centered celestial equatorial reference frame defined, for example, in Ref. [5]. To estimate the SME-coefficients, we fit this hypothetical signal for Lorentz violation to the experimental results shown in Fig. 2, weighted according to the inverse squared fit error. The results for the $\lambda^{IJ} \equiv (\tilde{\kappa}_{e-})^{IJ} + 2\mathcal{B}_q c_{IJ}$ (where $2\mathcal{B}_q = -5.92$ is a material parameter for fused quartz [8]) are, in parts in 10^{16},

$$\begin{aligned} \lambda^{XY} &= -4.9(2.5), \quad \lambda^{XZ} = -1.4(2.5), \\ \lambda^{YZ} &= 4.1(3.9), \quad \lambda^{ZZ} = 13.3(9.8), \\ \lambda^{XX} - \lambda^{YY} &= 05.7(22.6)\,. \end{aligned} \tag{5}$$

The results for $(\tilde{\kappa}_{o+})$ are, in parts in 10^{12},

$$\begin{aligned} (\tilde{\kappa}_{o+})^{XY} &= 5.7(3.7), \quad (\tilde{\kappa}_{o+})^{XZ} = 5.3(6.3), \\ (\tilde{\kappa}_{o+})^{YZ} &= -0.2(6.2). \end{aligned} \tag{6}$$

The Perth setup compares the frequencies of two orthogonally orientated high Q-factor (2×10^8) cryogenically cooled ($\sim 6\,\mathrm{K}$) microwave resonators. Each consists of a sapphire crystal mounted inside a metallic shield. The crystal is 3 cm diameter and height, and is machined with its crystal axis in line with the cylindrical axis. Each resonator is excited in the whispering gallery $\mathrm{WGH}_{8,0,0}$ mode at approximately 10 GHz by two separate Pound stabilized oscillator circuits, with a difference frequency of about 226 kHz. The $\mathrm{WGH}_{8,0,0}$ mode has dominant electric and magnetic fields in the axial and radial directions respectively, corresponding to a Poynting vector around the circumference. 98% of the electromagnetic energy is confined within the sapphire crystal so it is subject to the index of refraction of sapphire ($n_\perp = 3.04, n_\parallel = 3.37$ at 6 K). The two resonators are oriented with their cylindrical axis perpendicular to each other in the horizontal plane and placed inside a vacuum chamber and cryogenic dewar, which is mounted in a turntable and rotated at $1/(18\,\mathrm{s})$ about its vertical axis.

As discussed in a previous publication [16], the data used in this analysis spans a period from December 2004 to January 2006. It consists of 27 sets of data totalling approximately 121 days. The data analysis proceeds in analogy to the Berlin setup. The data is broken down into blocks of 40 rotations, each of which is fitted with $B(t_i)$ and $C(t_i)$. The hypothetical signal for Lorentz violation in the photon sector is listed in Tab. I of [16]. We calculate the effects of the Dirac sector as in [6, 8], taking into account both the changes in the geometry of the cavity and the index of refraction. We find that the combined signal can be expressed by substituting $(\tilde{\kappa}_{e-})^{IJ} \to \mu^{IJ} = (\tilde{\kappa}_{e-})^{IJ} + 3\mathcal{B}_\mathrm{s} c_{IJ}$ in that table, where $3\mathcal{B}_\mathrm{s} \equiv 3[-(\frac{1}{3} - \frac{1}{2}\mathcal{B}_{13}) + \bar{\beta}] \approx -2.25$ is a material and geometry-dependent coefficient for the sapphire WGR [8]. Fitting the hypothetical signal to the data leads to (parts in 10^{16})

$$\begin{aligned} \mu^{XY} &= 2.9(2.3), \quad \mu^{XZ} = -6.9(2.2), \\ \mu^{YZ} &= 2.1(2.1), \quad \mu^{ZZ} = 143(179), \\ \mu^{XX} - \mu^{YY} &= -5.0(4.7), \end{aligned} \tag{7}$$

and (parts in 10^{12})

$$\begin{aligned} (\kappa_{o+})^{XY} &= -0.9(2.6), \quad (\kappa_{o+})^{XZ} = -4.4(2.5), \\ (\kappa_{o+})^{YZ} &= -3.2(2.3). \end{aligned} \tag{8}$$

The data from both setups are of similar quality. However, the constraints on the $\tilde{\kappa}_{o+}$ from Perth have ~ 2 times lower confidence interval. On the other hand, λ^{ZZ} from the Berlin setup is about 17 times more accurate than μ^{ZZ} from Perth, as this signal occurs at $2\omega_r$, at which frequency signals from wobble of the

TABLE I: Signal components for the Berlin setup. $\lambda^2 \equiv \lambda^{XX} - \lambda^{YY}$.

C_0	$\frac{1}{4}\sin^2\chi(\frac{3}{2}\lambda^{ZZ} - \beta_\oplus[(\cos\eta\kappa_{o+}^{XZ} + 2\kappa_{o+}^{XY}\sin\eta)\cos\Omega_\oplus T' + \kappa_{o+}^{YZ}\sin\Omega_\oplus T']$	B_0	0
C_{s1}	$\frac{1}{2}\cos\chi\sin\chi(-\lambda^{YZ} + \beta_\oplus[\kappa_{o+}^{XY}\cos\eta - \kappa_{o+}^{XZ}\sin\eta]\cos\Omega_\oplus T'$	B_{s1}	$-C_{c1}/\cos\chi$
C_{c1}	$\frac{1}{2}\cos\chi\sin\chi(-\lambda^{XZ} + \beta_\oplus[\kappa_{o+}^{YZ}\sin\eta\cos\Omega_\oplus T' - \kappa_{o+}^{XY}\sin\Omega_\oplus T']$	B_{c1}	$C_{s1}/\cos\chi$
C_{s2}	$\frac{1}{4}(1+\cos^2\chi)(\lambda^{XY} - \beta_\oplus[\kappa_{o+}^{YZ}\cos\eta\cos\Omega_\oplus T' + \kappa_{o+}^{XZ}\sin\Omega_\oplus T']$	B_{s2}	$-2\cos\chi/(1+\cos^2\chi)C_{c2}$
C_{c2}	$\frac{1}{4}(1+\cos^2\chi)(\frac{1}{2}\lambda^2 - \beta_\oplus[\kappa_{o+}^{XZ}\cos\eta\cos\Omega_\oplus T' - \kappa_{o+}^{YZ}\sin\Omega_\oplus T'])$	S_{c2}	$2\cos\chi/(1+\cos^2\chi)C_{s2}$

TABLE II: Results on electron and photon coefficients $\tilde{\kappa}_{e-}$ and c in units of 10^{-16} and $\tilde{\kappa}_{o+}$ in 10^{-12} (one sigma errors).

$\tilde{\kappa}_{e-}^{XX} - \tilde{\kappa}_{e-}^{YY}$	$\tilde{\kappa}_{e-}^{XY}$	$\tilde{\kappa}_{e-}^{XZ}$	$\tilde{\kappa}_{e-}^{YZ}$	$\tilde{\kappa}_{e-}^{ZZ}$
−12(16)	7.7(4.0)	−10.3(3.9)	0.9(4.2)	223(290)
$c_{XX} - c_{YY}$	$c_{(XY)}$	$c_{(XZ)}$	$c_{(YZ)}$	c_3
−2.9(6.3)	2.1(0.9)	−1.5(0.9)	−0.5(1.2)	−106(147)
λ^{ZZ}	$\tilde{\kappa}_{o+}^{XY}$	$\tilde{\kappa}_{o+}^{XZ}$	$\tilde{\kappa}_{o+}^{YZ}$	
13.3(9.8)	1.7(2.0)	-3.1(2.3)	-2.8(2.2)	

turntable have a strong Fourier component. The precision turntable along with an active vertical alignment of the rotation axis leads to this higher accuracy.

Combined, the constraints from both setups, shown in Eqs. (3-6), are sufficient to calculate separate bounds on Lorentz violation in the electron and photon sector, see Tab. II. We also included the limit on λ^{ZZ} from the Berlin setup. For the elements of κ_{o+}, the two experiments provide complementary limits. The ones listed in the table are obtained from both by weighted averaging. We note that $\tilde{\kappa}_{e-}^{XZ}$ and c_{XY} are at the (2-3)σ level. However, systematic effects associated with rotation of the turntable are extremely hard to quantify at this level, since with the given noise of the data this takes a full year of averaging. To enable a better characterization of the systematics or of a possible signal, lower noise is required. This will be achieved in the next generation of rotating experiments with cavities having even higher quality factors, which promise to reduce the noise by more than one order of magnitude. Therefore, for the time being, we regard our results as a confirmation of Lorentz Invariance. In the future, birefringence- [8] or dual-mode- [22] cavity experiments can overcome some of the systematic effects.

In summary, we present relativity tests based on simultaneous, complementary Michelson-Morley experiments. Use of dissimilar cavities, operation on both hemispheres, and extensive data-taking over a period of > 1 y makes this the first simultaneous measurement of a complete set of limits on spin-independent Lorentz violation in the electron and photon sectors. We determine 14 limits on Lorentz violation parameters of the standard model extension. Compared to the best previous limits that do not use assumptions on the vanishing of Lorentz violation in one sector [8, 11, 12, 21], they are improved by factors between $\sim 3 - 50$. Thus, we also confirm the isotropy of the velocity of light without using such assumptions.

We would like to thank S. Chu and G. Ertl for support and important discussions. This work was supported by the Australian Research Council. H.M. thanks the Alexander von Humboldt Foundation and S.H. the Studienstiftung des Deutschen Volkes.

[1] C.M. Will, *Theory and experiment in gravitational physics (revised edition)*, (University Press, Cambridge, 1993)

[2] G. Amelino-Camelia, C. Lämmerzahl, A. Macias, and H. Müller in: A.Macias, C. Lämmerzahl, and D. Nunez (eds.), Gravitation and Cosmology, page 30. AIP Conference Proceedings **758**, Melville, N.Y. (2005).

[3] D. Mattingly, Living Reviews **8,** http://www.livingreviews.org/lrr20055, 2005 (cited on April 4, 2006).

[4] A.A. Michelson, Am. J. Sci. **22**, 120 (1881); A.A. Michelson and E.W. Morley, Am. J. Sci **34**, 333 (1887); Phil. Mag. **24**, 449 (1897)

[5] V.A. Kostelecký and M. Mewes, Phys. Rev. D **66**, 056005 (2002); Phys. Rev. Lett. **97,** 140401 (2006).

[6] H. Müller, C. Braxmaier, S. Herrmann, A. Peters, and C. Lämmerzahl, Phys. Rev. D **67,** 056006 (2003).

[7] H. Müller, S. Herrmann, A. Saenz, A. Peters, and C. Lämmerzahl, Phys. Rev. D **68,** 116006 (2003).

[8] H. Müller, Phys. Rev. D **71,** 045004 (2005).

[9] A. Brillet and J.L. Hall, Phys. Rev. Lett. **42,** 549 (1979).

[10] D. Hils and J.L. Hall, Phys. Rev. Lett. **64,** 1697 (1990); C. Braxmaier *et al., ibid.* **88,** 010401 (2001); H. Müller *et al.,* Int. J. Mod. Phys. D **11**, 1101 (2002); P. Wolf *et al.,* Phys. Rev. Lett. **90**, 060402 (2003).

[11] C. Braxmaier, H. Müller, O. Pradl, J. Mlynek, A. Peters, and S. Schiller, Phys. Rev. Lett. **88,** 010401 (2002); H. Müller, S. Herrmann, C. Braxmaier, S. Schiller, and A. Peters, *ibid.* **91,** 020401 (2003); Appl. Phys. B (laser opt.) **77,** 719 (2003); H. Müller *et al.,* Opt. Lett. **28,** 2186 (2003).

[12] P. Wolf *et al.,* Gen. Relativ. Gravitat. **36,** 2351 (2004); Phys. Rev. D **70**, 051902(R) (2004).

[13] P. Antonini *et al.*, Phys. Rev. A **71,** (R), 050101 (2005).

[14] S. Herrmann, A. Senger, E. Kovalchuk, H. Müller, and A. Peters, Phys. Rev. Lett. **95,** 150401 (2005).

[15] P.L. Stanwix *et al.,* Phys. Rev. Lett. **95,** 040404 (2005).

[16] P.L. Stanwix, M.E. Tobar, P. Wolf, C.R. Locke, and E.N. Ivanov, Phys. Rev. D **74,** 081101(R) (2006).

[17] J.A. Lipa, J.A. Nissen, S. Wang, D.A. Stricker, and D. Avaloff, Phys. Rev. Lett. **90,** 060403 (2003).

[18] D. Colladay and V.A. Kostelecký, Phys. Rev. D **55**, 6760

(1997); Phys. Rev. D **58**, 116002 (1998); V.A. Kostelecký, Phys. Rev. D 69, 105009 (2004).
[19] W.-T. Ni, Phys. Rev. Lett. **38,** 301 (1977).
[20] H. Müller, S. Herrmann, A. Saenz, A. Peters, and C. Lämmerzahl, Phys. Rev D **70,** 076004 (2004).
[21] B. Altschul, Phys. Rev. Lett. **96,**, 201101 (2006).
[22] M.E. Tobar *et al.,* Springer Lect. Notes Phys. **702** 416-450 (2006).